Journal of proteome research

Article

pubs.acs.org/jpr

Combined Clinical Phenotype and Lipidomic Analysis Reveals the Impact of Chronic Kidney Disease on Lipid Metabolism

Hua Chen,[†,@] Lin Chen,[†,@] Dan Liu,[†] Dan-Qian Chen,[†] Nosratola D. Vaziri,[‡] Xiao-Yong Yu,[§] Li Zhang,[∥] Wei Su,[⊥] Xu Bai,[#] and Ying-Yong Zhao*[,†]

[†]Key Laboratory of Resource Biology and Biotechnology in Western China, Ministry of Education, School of Life Sciences, Northwest University, No. 229 Taibai North Road, Xi'an, Shaanxi 710069, China

[‡]Division of Nephrology and Hypertension, School of Medicine, University of California Irvine, MedSci 1 C352, Irvine, California 92897, United States

[§]Department of Nephrology, Affiliated Hospital of Shaanxi Institute of Traditional Chinese Medicine, No. 2 Xihuamen, Xi'an, Shaanxi 710003, China

[∥]Department of Nephrology, Xi'an No. 4 Hospital, No. 2 Jiefang Road, Xi'an, Shaanxi 710004, China

[⊥]Department of Nephrology, Baoji Central Hospital, No. 8 Jiangtan Road, Baoji, Shaanxi 721008, China

[#]Solution Centre, Waters Technologies (Shanghai) Ltd., No. 1000 Jinhai Road, Shanghai 201203, China

Supporting Information

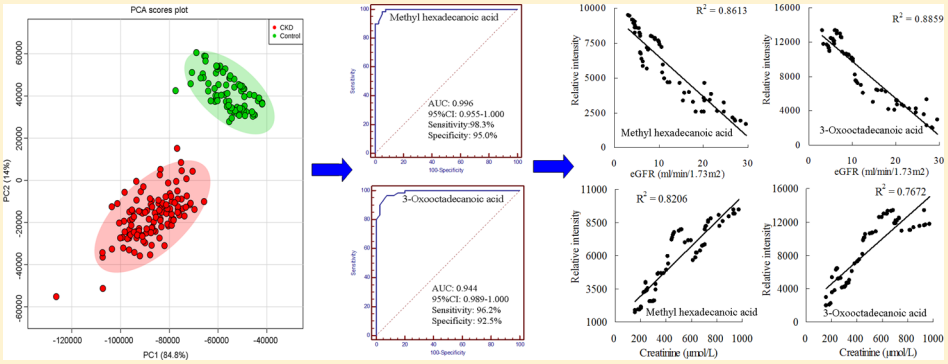

ABSTRACT: Chronic kidney disease (CKD) results in significant dyslipidemia and profound changes in lipid and lipoprotein metabolism. The associated dyslipidemia, in turn, contributes to progression of CKD and its cardiovascular complications. To gain an in-depth insight into the disorders of lipid metabolism in advanced CKD, we applied UPLC-HDMS-based lipidomics to measure serum lipid metabolites in 180 patients with advanced CKD and 120 age-matched healthy controls. We found significant increases in the levels of total free fatty acids, glycerolipids, and glycerophospholipids in patients with CKD. The levels of free fatty acids, glycerolipids, and glycerophospholipids directly correlated with the level of serum triglyceride and inversely correlated with the levels of total cholesterol and eGFR. A total of 126 lipid species were identified from positive and negative ion modes. Out of 126, 113 identified lipid species were significantly altered in patients with CKD based on the adjusted FDR method. These results pointed to profound disturbance of fatty acid and triglyceride metabolisms in patients with CKD. Logistic regression analysis showed strong correlations between serum methyl hexadecanoic acid, LPC(24:1), 3-oxooctadecanoic acid, and PC(20:2/24:1) levels with eGFR and serum creatinine levels (R > 0.8758). In conclusion, application of UPLC-HDMS-based lipidomic technique revealed profound changes in lipid metabolites in patients with CKD. The observed increases in serum total fatty acids, glycerolipids, and glycerophospholipids levels directly correlated with increased serum triglyceride level and inversely correlated with the eGFR and triglyceride levels.

KEYWORDS: *chronic kidney disease, lipidomics, lipid metabolism, fatty acid metabolism, triglyceride metabolism, glomerular filtration rate*

1. INTRODUCTION

By promoting tubulo-interstitial fibrosis and glomerulosclerosis the fibrotic process constitutes the final pathway in progression of all forms of chronic kidney disease (CKD). Renal fibrosis is characterized by myofibroblasts transformation, accumulation of fibrillary collagen, loss of capillary network, and inflammatory cell infiltration.[1] Earlier studies have demonstrated the role of lipid mediators in progression of CKD.[2−5] In fact, recent in vivo and in vitro studies demonstrated the role of impaired fatty acid

Received: November 4, 2016
Published: March 13, 2017

DOI: 10.1021/acs.jproteome.6b00956
J. Proteome Res. 2017, 16, 1566−1578

oxidation, depressed mitochondrial ATP generation, and enhanced reactive oxygen species production in the pathogenesis of oxidative stress, tubular epithelial cell death, and interstitial inflammation and fibrosis.[6]

Different kidney diseases result in marked alterations of lipid metabolism and serum lipid profile.[7] The associated lipid disorders, in turn, contribute to progression of kidney disease and its numerous comorbidities including cardiovascular disease, impaired energy metabolism, diminished exercise capacity, and various other complications. Severity of renal failure and presence and severity of proteinuria independently impact the nature of lipid disorders in patients with kidney disease.[8] In addition, dietary and drug regimens and renal replacement therapies (i.e., hemodialysis, peritoneal dialysis, and renal transplantation) significantly affect the lipid profile in this population.[9,10]

Although the nature and mechanisms of the abnormalities of serum lipid and lipoproteins in CKD and nephrotic syndrome are well-known, their effect on the lipid metabolites have not been fully elucidated. In the past several years, lipidomics has been increasingly used to determine the changes of lipid metabolites and identify the biomarker of various diseases in animal and humans.[11,12] Ultra performance liquid chromatography-quadrupole time-of-flight high-definition mass spectrometry (UPLC-QTOF/HDMS) has been increasingly applied to lipidomics.[13−17] A large number of clinical studies demonstrated that abnormal lipid metabolism and serum lipid profile may contribute to the pathogenesis and progression of CKD, and a few studies have addressed the lipidomic profile of kidney diseases using untargeted lipidomic approach.[18] Lipidomic studies have demonstrated remarkable elevation of serum free fatty acid (FFA), saturated FFA, eicosanoid, lysophosphatidyl ethanolamine, and lysophosphatidyl inositol levels in prehemodialysis patients compared to the healthy controls.[19] Lipidomics has been applied to the determination of the lipid profile of low density lipoprotein (LDL), which showed significant increases in triacylglycerides and significant decreases in phosphatidylcholines, plasmenyl ethanolamines, sulfatides, ceramides, and cholesterol sulfate in patients with advanced CKD.[20] In the present study, we conducted an untargeted serum lipidomic analysis in a group of patients with advanced CKD and a group of healthy controls using UPLC-QTOF/HDMS.

2. METHODS

2.1. Chemicals and Reagents

Ostro 96-well plate was provided by Waters Technologies (Shanghai) Ltd. (Shanghai, China). Formic acid and ammonium formate were purchased from Sigma Chemical Co., Ltd. (Sigma Corp., St. Louis, MO). LC-grade chloroform, methanol, 2-propanol, and acetonitrile were purchased from the Baker Chemical Co. (Phillipsburg, NJ). Lipid analytical standards were purchased from the Avanti polar lipids Inc. (Alabaster, Alabama). Ultra purity water was prepared using a Milli-Q water purification system (Billerica, MA). Other chemicals were of analytical grade, and their purity was above 99.5%.

2.2. Participants

In this cross-sectional study, patients with CKD were recruited at the Xi'an Fourth Hospital and the Traditional Chinese Medicine Hospital between February 2013 and November 2014. Serum from a total of 200 adult individuals (>18 years old), including 120 patients and 80 healthy controls, were collected for the discovery phase and from an additional 100 individuals, including 60 patients and 40 healthy controls for the validation phase. Patients with stage 4 and 5 were referred by nephrologists and were diagnosed based on clinical criteria (i.e., kidney damage, reduced estimated glomerular filtration rate (eGFR) for at least 3 months, and in some cases kidney biopsy). Patients with acute kidney injury, liver disease, patients treated with immunosuppressive agents in the past six months, or chemotherapy within the past two years, as well as patients undergoing chronic dialysis or kidney transplantation were excluded. The underlying causes of CKD were hypertension (n = 100), chronic tubulointerstitial nephritis (n = 22), chronic glomerulonephritis (n = 42), and obstructive uropathy (n = 16). To isolate the effects of CKD from those caused by systemic disorders, patients with diabetes, lupus erythematosus, amyloidosis etc. were excluded from the study. The study was approved by the Ethical Committee, and all patients had been given written informed consent prior to entering the study.

2.3. Demographics and Medical Information

Baseline information included sex, age, body mass index (BMI), blood pressure, primary renal diseases, and medication histories. Blood samples were obtained after an overnight fasting. Serum was immediately separated by centrifugation and stored at −80 °C. The eGFR was calculated using the modified equation of Diet of Renal Disease. Serum biochemistry was determined by Olympus AU640 automatic analyzer. Serum high sensitivity C-reactive protein (CRP) was measured by an automated immunoturbidimetric assay. Serum interleukin-6 and tumor necrosis factor-α (TNF-α) were measured using the commercially available ELISA kits.

2.4. Lipid Profiling

UPLC-HDMS was used for the determination of lipid profile of all samples. The lipid profile procedure including sample preparation, lipid separation, lipid detection, data preprocessing, and statistical analysis for lipid identification was performed following our published protocols with minor modifications.[21] Briefly, serum total lipids were extracted using Ostro 96-well plate. One hundred microliters of serum sample was loaded into each well in Ostro preparation plate fitted onto a vacuum manifold. Three hundred microliters of elution solvent (1:1, $CHCl_3/CH_3OH$) was added to each well and mixed aspirating the mixture 10× by a micropipette. A vacuum of approximately 15″ Hg was used to the plate until the solvent was drained. This step was repeated 3 times and obtained the total extract to approximately 900 μL. The eluate fraction was dried down under nitrogen and reconstituted with 200 μL 1:1 (v/v) $CHCl_3/CH_3OH$. The extracted sample was then injected into the UPLC-HDMS system. Chromatographic separation was carried out at 45 °C on an ACQUITY UPLC HSS T3 column (2.1 × 100 mm, 1.8 μm, UK). A gradient of 10 mM ammonium formate in 2-propanol/acetonitrile (90/10) in 0.1% formic acid and 10 mM ammonium formate in ACN/H_2O (60/40) in 0.1% formic acid was used as follows: a linear gradient from 0 to 10 min, 35.0−99.0% A, and from 10.0 to 12.0 min, 99.0−35.0% A. The flow rate was 0.5 mL/min. The temperatures of the autosampler and column were maintained at 4 and 55 °C, respectively. Every 5 μL sample solution was injected for each run. Mass spectrometry was carried out by a Xevo G2 QTof. The scan range was from 100 to 1500 m/z in both positive and negative ion modes, the cone and capillary voltages were set at 60 V and 3.0 kV, respectively. The desolvation gas and cone gas was set to 900 L/h and 50 L/h, respectively. The gas temperature

DOI: 10.1021/acs.jproteome.6b00956
J. Proteome Res. 2017, 16, 1566−1578

Table 1. Summary of Clinical and Demographic Baseline Characteristics of Patients with CKD and Healthy Controls in This Study[a]

	discover phase		validation phase	
clinical characteristics	healthy controls	patient with CKD	healthy controls	patient with CKD
male/female	45/35	70/50	23/17	35/25
age (years)	55.7 ± 11.2	57.3 ± 14.5	54.1 ± 9.6	57.1 ± 15.8
body mass index (kg/m2)	24.3 ± 3.5	25.4 ± 5.2	23.3 ± 2.8	25.9 ± 4.9
SBP (mm Hg)	121.7 ± 12.6	144.2 ± 15.2[c]	119.5 ± 13.3	141.2 ± 16.8[c]
DBP (mm Hg)	75.1 ± 11.3	82.4 ± 12.5[c]	74.6 ± 10.3	83.7 ± 10.8[c]
eGFR (mL/min/1.73m2)	99.5 ± 15.1	14.4 ± 5.1[c]	97.4 ± 23.2	13.2 ± 4.2[c]
BUN (mmol/L)	5.11 ± 1.05	33.0 ± 16.2[c]	5.06 ± 0.87	34.6 ± 17.6[c]
serum creatinine (μmol/L)	68.7 ± 14.1	516 ± 208[c]	73.8 ± 17.2	486 ± 216[c]
serum albumin (g/L)	47.3 ± 3.7	35.9 ± 6.7[c]	47.5 ± 2.3	36.7 ± 5.5[c]
HDL-cholesterol (mmol/L)	1.32 ± 0.68	1.14 ± 0.53*	1.41 ± 0.64	1.24 ± 0.48*
LDL-cholesterol (mmol/L)	2.85 ± 1.03	3.16 ± 1.09*	2.89 ± 1.05	3.19 ± 1.04*
triglycerides (mmol/L)	1.62 ± 0.53	1.91 ± 0.67[b]	1.63 ± 0.46	1.90 ± 0.72[b]
VLDL-cholesterol (mmol/L)	0.32 ± 0.08	0.34 ± 0.14	0.34 ± 0.09	0.33 ± 0.13
urine proteins (g/24h)	N/A	1.89 ± 1.38[c]	N/A	1.80 ± 1.47[c]
high sensitive CRP (mg/L)	1.19 ± 0.75	4.15 ± 1.42[c]	1.22 ± 0.72	3.97 ± 1.18[c]
interleukin-6 (pg/mL)	1.32 ± 0.34	2.52 ± 0.77[c]	1.35 ± 0.41	2.61 ± 0.81[c]
TNF-γ (pg/mL)	1.46 ± 0.45	2.42 ± 0.86[c]	1.51 ± 0.56	2.34 ± 0.79[c]

[a]Results are expressed as the means ± standard deviation. [b]**$P < 0.01$. [c]***$P < 0.001$ compared with healthy controls. N/A, not available.

and source temperature was set to 500 and 120 °C, respectively. Waters Unifi software was used for the data acquisition and analysis.

2.5. Data Analysis, Model Development, Lipid Selection, and Cross Validation

The raw data from UPLC-HDMS were first preprocessed by Progenesis QI (Waters, Manchester, U.K.). Principal component analysis (PCA) and orthogonal partial least-squares-discriminant analysis (OPLS-DA) were performed to discriminate between patients with CKD and healthy controls. The variables were selected based on variable importance in the projection (VIP > 1.0) from the peak intensity. We reduced the resulting matrix by removing any ion peaks with zero value in the samples to obtain consistent differential variables. Variables were selected by one-way analysis of variance (ANOVA) with a threshold of $P < 0.05$ in SPSS 19.0. On the basis of previous literature, the variables were identified and confirmed by comparing MS data, MS/MS fragments, molecular weights, and elemental compositions with the available reference chemicals.[22,23]

Identified lipids were subjected to further statistical analysis by univariate and multivariate statistical methods. Fold change (FC) was calculated based on mean ratios for CKD/controls. Lipids were also selected by Mann−Whitney U test with a threshold of $P < 0.05$. The resultant P values from ANOVA were further adjusted by a false discovery rate (FDR) based on the Hochberg-Benjamini method. Significantly altered variables were defined and further identified by a VIP > 1.0, $P < 0.05$, and FDR < 0.05. Variables or lipids are visualized using heatmap and z-score plots analyses. The z-score of lipids was calculated according to reference distribution of the control samples. Then each lipid was centered by the control mean and scale by the control standard deviation. Pearson correlation coefficient was performed to find the correlations between the potential lipids.

2.6. Binary Logistic Regression (BLR) and Receiver Operating Characteristics (ROC) Curve Analysis

BLR and ROC curve were performed by SPSS software. On the basis of the binary outcome of patients with CKD and healthy controls as dependent variables, we developed a BLR model to find the best combination of significantly altered lipid species. The methods of the forward stepwise regression and Wald test were used for selecting altered lipid classes and assessing significance in BLR prediction model, respectively. The method was used to discover the most important lipid species until there were no more significant predictors from the data. The Wald test provided a P value to each individual lipid species to assess their significance. PLS-DA-based ROC analysis was performed for evaluating significantly altered lipid species using MedCalc 14.0.

3. RESULTS

3.1. General Data

To isolate the effects of CKD from those caused by systemic disorders, patients with diabetes, systemic lupus erythematosus, amyloidosis, etc. were excluded from the study. The general clinical and demographic data are presented in Table 1. There were no significant differences in age and BMI between the two groups. Patients with CKD had higher SBP and DBP and lower eGFR compared to the healthy controls. Serum creatinine, BUN, LDL-C, and triglycerides were significantly increased, and serum HDL-C was significantly decreased in patients with CKD compared to the healthy controls. Patients with CKD had higher serum CRP, IL-6, and TNF-α levels.

3.2. Selection and Identification of Significantly Altered Lipid Classes

To evaluate the changes of lipidome in patients with CKD and find significantly altered lipid species, a two-predictive component OPLS-DA was performed using data from patients with CKD and healthy controls. The OPLS-DA score plots could readily be divided into two clusters, indicating that serum lipid metabolic patterns were significantly altered in patients with CKD (Figure S1). Initially, 287 and 196 variables were selected according to the VIP values from S-plots, respectively (Figure S1). On the basis of authentic standards, analogue structure of authentic chemicals or databases, 77 and 49 lipid species were identified from positive ion mode and negative ion

DOI: 10.1021/acs.jproteome.6b00956
J. Proteome Res. 2017, 16, 1566−1578

Table 2. Plasma Differential Lipid Species in Patients with CKD Compared with Healthy Controls

no.	lipid	VIP[a]	FC[b]	P[c]	FDR[d]	AUC	95% CI	sensitivity (%)	specificity (%)
1	PG(16:0/16:1)[e]	16.8	7.96	4.04×10^{-98}	4.24×10^{-97}	1.00	0.982−1.00	100	100
2	LPC(24:1)[g]	14.0	7.87	8.59×10^{-98}	8.32×10^{-97}	1.00	0.982−1.00	100	100
3	PE(P-18:1/14:1)[e]	12.8	8.89	1.80×10^{-99}	7.58×10^{-98}	1.00	0.982−1.00	100	100
4	PE(16:1/18:1)[e]	9.81	10.97	2.34×10^{-99}	7.38×10^{-98}	1.00	0.982−1.00	100	100
5	LSM(d18:0)[e]	6.42	13.31	9.98×10^{-99}	1.26×10^{-97}	1.00	0.982−1.00	100	100
6	MG(20:4)[e]	6.01	11.15	1.10×10^{-99}	1.39×10^{-97}	1.00	0.982−1.00	100	100
7	DG(18:3/22:6)[e]	5.63	14.24	3.23×10^{-88}	2.26×10^{-87}	1.00	0.980−1.00	100	98.0
8	LPC(20:4)[f]	5.54	13.33	8.00×10^{-89}	6.30×10^{-88}	1.00	0.982−1.00	100	100
9	PA(16:0/18:2)[e]	4.52	25.77	4.82×10^{-73}	2.64×10^{-72}	1.00	0.982−1.00	100	100
10	PE(22:4/P-18:0)[e]	4.44	10.44	1.75×10^{-73}	1.00×10^{-72}	1.00	0.982−1.00	100	100
11	docosatrienoic acid[f]	3.85	9.89	3.70×10^{-95}	3.11×10^{-94}	1.00	0.982−1.00	100	100
12	LPE(18:0)[f]	3.77	7.96	6.75×10^{-99}	1.06×10^{-97}	1.00	0.982−1.00	100	100
13	LPE(22:4)[f]	3.55	9.32	5.89×10^{-97}	5.30×10^{-96}	1.00	0.858−0.943	100	90.0
14	methyl hexadecanoic acid[g]	3.24	3.46	1.33×10^{-10}	1.92×10^{-10}	0.89	0.982−1.00	100	100
15	LPE(24:1)[f]	3.13	9.49	1.40×10^{-98}	1.61×10^{-97}	1.00	0.982−1.00	100	100
16	PGP(18:0/18:1)[e]	2.71	9.6	4.46×10^{-99}	9.36×10^{-98}	1.00	0.982−1.00	100	100
17	PE(18:4/14:0)[e]	2.42	27.21	1.74×10^{-56}	7.05×10^{-56}	1.00	0.982−1.00	100	100
18	chenodeoxycholic acid sulfate[f]	2.34	12.3	5.74×10^{-67}	2.89×10^{-66}	1.00	0.980−1.00	98.3	98.7
19	PGP(18:3/22:5)[e]	2.13	8.39	3.04×10^{-99}	7.67×10^{-98}	1.00	0.982−1.00	100	100
20	PG(18:0/20:3)[e]	2.07	3.95	3.04×10^{-62}	1.37×10^{-61}	1.00	0.982−1.00	100	100
21	eicosatrienoic acid[f]	2.04	0.23	7.12×10^{-75}	4.27×10^{-74}	1.00	0.982−1.00	100	100
22	DG(20:4/20:5)[e]	1.92	9.17	5.91×10^{-80}	3.73×10^{-79}	1.00	0.982−1.00	100	100
23	DG(22:5/18:4)[e]	1.91	16.48	5.93×10^{-99}	1.07×10^{-97}	1.00	0.982−1.00	100	100
24	palmitic acid[g]	1.85	13.93	1.76×10^{-57}	7.40×10^{-57}	1.00	0.982−1.00	100	100
25	PC(22:0/24:0)[e]	1.83	14.41	6.38×10^{-63}	2.98×10^{-62}	1.00	0.980−1.00	100	98.0
26	3-hydroxytetradecanedioic acid[f]	1.82	17.66	7.79×10^{-67}	3.77×10^{-66}	1.00	0.982−1.00	100	100
27	LPC(14:0)[g]	1.81	0.64	1.88×10^{-28}	4.08×10^{-28}	0.92	0.878−0.975	89.2	87.5
28	PG(16:0/20:3)[e]	1.64	18.63	2.13×10^{-88}	1.58×10^{-87}	1.00	0.982−1.00	100	100
29	PC(18:2/22:0)[e]	1.55	15.53	1.69×10^{-99}	1.06×10^{-97}	1.00	0.980−1.00	100	98.0
30	DG(22:5/20:4)[e]	1.52	18.84	5.63×10^{-85}	3.73×10^{-84}	1.00	0.982−1.00	100	100
31	9-oxooctadecanoic acid[f]	1.43	12.49	7.46×10^{-26}	1.52×10^{-25}	1.00	0.973−1.00	99.2	98.7
32	TG(14:1/20:0/20:3)[e]	1.34	2.62	1.49×10^{-24}	2.80×10^{-24}	0.92	0.873−0.953	87.5	87.5
33	TG(15:0/20:1/15:0)[e]	1.32	9.19	6.96×10^{-56}	2.74×10^{-55}	1.00	0.982−1.00	100	100
34	LPC(18:2)[e]	1.23	20.21	7.61×10^{-99}	1.07×10^{-97}	1.00	0.982−1.00	100	100
35	12-hydroxyheptadecanoic acid[f]	1.21	6.83	1.45×10^{-55}	5.54×10^{-55}	1.00	0.978−1.00	98.3	100
36	MG(18:4)[f]	1.15	15.09	2.20×10^{-48}	7.51×10^{-48}	1.00	0.982−1.00	100	100
37	MG(20:5)[f]	1.13	8.19	7.36×10^{-69}	3.86×10^{-68}	1.00	0.979−1.00	98.3	98.7
38	18-hydroxyarachidonic acid[f]	8.54	0.66	6.59×10^{-47}	2.19×10^{-46}	0.98	0.948−0.994	90.0	96.2
39	3-oxooctadecanoic acid[g]	7.41	3.97	1.03×10^{-33}	2.61×10^{-33}	0.98	0.943−0.992	91.7	100
40	arachidonic acid[g]	4.86	0.13	1.92×10^{-28}	4.11×10^{-28}	0.98	0.952−0.995	94.2	98.7
41	DG(20:1/22:2)[e]	4.54	0.18	1.28×10^{-54}	4.75×10^{-54}	0.99	0.960−0.998	100	100
42	2-arachidonylglycerol[e]	4.15	0.63	8.59×10^{-50}	3.01×10^{-49}	0.98	0.952−0.995	89.2	100
43	TG(18:4/20:4/22:6)[e]	3.08	4.12	7.73×10^{-46}	2.50×10^{-45}	0.99	0.958−0.997	91.7	97.5
44	TG(14:1/14:0/16:1)[e]	2.78	0.66	1.18×10^{-42}	3.63×10^{-42}	0.96	0.927−0.985	89.2	93.7
45	PC(20:2/24:1)[f]	2.53	0.62	8.46×10^{-35}	2.37×10^{-34}	0.95	0.904−0.973	87.5	93.7
46	TG(22:0/22:4/14:1)[e]	2.11	8.61	3.85×10^{-34}	1.03×10^{-33}	0.95	0.906−0.974	88.3	100
47	DG(20:0/18:3)[e]	1.98	0.32	1.06×10^{-11}	1.59×10^{-11}	0.92	0.874−0.954	85.8	92.5
48	PE(24:1/24:1)[e]	1.69	1.73	4.30×10^{-29}	9.84×10^{-29}	0.94	0.893−0.966	91.7	93.7
49	DG(22:0/15:0)[e]	1.64	0.10	4.35×10^{-50}	1.57×10^{-49}	0.99	0.961−0.998	98.3	98.7
50	bisnorcholic acid[e]	1.53	0.74	3.49×10^{-34}	9.57×10^{-34}	0.95	0.905−0.973	90.8	88.7
51	MG(14:0)[f]	1.32	0.16	4.02×10^{-42}	1.21×10^{-41}	0.98	0.950−0.995	94.2	97.5
52	TG(22:2/22:5/22:6)[e]	1.28	6.20	6.05×10^{-34}	1.56×10^{-33}	0.95	0.915−0.978	90.0	100
53	prostaglandin E2[g]	1.25	0.16	3.54×10^{-23}	6.55×10^{-23}	0.98	0.944−0.993	95.8	97.5
54	DG(20:1/22:5)[e]	1.23	2.62	4.61×10^{-39}	1.35×10^{-38}	0.99	0.961−0.998	95.8	97.5
55	DG(22:5/22:0)[e]	1.22	0.09	1.06×10^{-35}	3.04×10^{-35}	0.96	0.923−0.983	93.3	95.0
56	PG(18:1/18:2)[e]	1.21	11.33	2.14×10^{-15}	3.29×10^{-15}	1.00	0.978−1.000	98.3	98.7
57	PE(24:1/18:1)[e]	1.20	6.66	2.52×10^{-31}	6.10×10^{-31}	0.98	0.945−0.993	95.8	98.7
58	TG(18:3/22:4/22:5)[e]	1.18	6.15	2.39×10^{-20}	4.01×10^{-20}	0.94	0.892−0.966	87.5	91.7
59	8,9-Epoxyeicosatrienoic acid[e]	1.17	0.67	1.02×10^{-57}	4.43×10^{-57}	1.00	0.978−1.000	97.5	100
60	chenodeoxycholic acid[g]	1.17	0.16	1.10×10^{-27}	2.32×10^{-27}	0.94	0.901−0.971	85.0	91.2
61	leukotriene B4[g]	1.12	0.17	5.94×10^{-43}	1.87×10^{-42}	0.98	0.948−0.994	95.0	97.5

DOI: 10.1021/acs.jproteome.6b00956
J. Proteome Res. 2017, 16, 1566−1578

Table 2. continued

no.	lipid	VIP[a]	FC[b]	P[c]	FDR[d]	AUC	95% CI	sensitivity (%)	specificity (%)
62	leukotriene A4[f]	1.11	0.66	1.06×10^{-25}	2.05×10^{-25}	0.97	0.933−0.988	91.7	98.7
63	PG(18:0/22:4)[e]	1.09	9.04	1.50×10^{-28}	3.31×10^{-28}	0.92	0.872−0.952	90.0	93.7
64	DG(15:0/18:0)[e]	1.05	0.28	8.64×10^{-04}	1.02×10^{-03}	0.91	0.858−0.943	87.5	88.7
65	PC(22:0/14:0)[e]	1.32	0.39	3.59×10^{-31}	8.53×10^{-31}				
66	PC(o-18:1/18:2)[e]	1.26	0.59	3.17×10^{-22}	5.48×10^{-22}				
67	TG(18:4/20:4/20:5)[e]	6.26	0.79	1.24×10^{-22}	2.23×10^{-22}				
68	TG(24:0/20:4/22:4)[e]	5.52	0.77	1.13×10^{-28}	2.54×10^{-28}				
69	TG(18:3/18:3/20:5)[e]	4.69	0.79	2.20×10^{-22}	3.90×10^{-22}				
70	ceramide(d18:1/16:0)[e]	4.44	0.33	8.38×10^{-26}	1.65×10^{-25}				
71	TG(18:4/18:4/20:5)[e]	3.26	3.31	9.72×10^{-20}	1.61×10^{-19}				
72	LPE(22:1)[e]	2.67	0.39	1.81×10^{-18}	2.89×10^{-18}				
73	PC(24:0/24:0)[e]	2.62	0.52	9.23×10^{-23}	1.69×10^{-22}				
74	Cer(t18:0/16:0)[e]	2.31	0.31	1.70×10^{-21}	2.90×10^{-21}				
75	PE(24:1/22:2)[e]	1.97	0.52	2.72×10^{-22}	4.76×10^{-22}				
76	MG(20:3)[e]	1.87	0.77	1.09×10^{-26}	2.25×10^{-26}				
77	TG(24:0/18:3/20:1)[e]	1.86	0.26	3.86×10^{-10}	5.46×10^{-10}				
78	TG(12:0/12:0/12:0)[e]	1.86	0.32	2.68×10^{-11}	3.97×10^{-11}				
79	DG(14:1/18:1)[e]	1.54	0.54	6.96×10^{-32}	1.72×10^{-31}				
80	TG(20:3/22:5/22:4)[e]	1.44	0.63	5.86×10^{-34}	1.54×10^{-33}				
81	LPE(16:1)[f]	1.39	0.30	3.18×10^{-19}	5.20×10^{-19}				
82	TG(15:0/20:5/22:6)[e]	1.38	1.53	6.86×10^{-18}	1.08×10^{-17}				
83	DG(20:3/16:0)[e]	1.34	0.21	8.91×10^{-07}	1.13×10^{-06}				
84	DG(15:0/20:0)[e]	1.28	0.26	2.94×10^{-07}	3.81×10^{-07}				
85	PG(18:1/18:0)[e]	1.18	0.73	8.72×10^{-25}	1.66×10^{-24}				
86	tetracosahexaenoic acid[g]	1.16	0.45	7.61×10^{-26}	1.52×10^{-25}				
87	taurocholic acid 3-sulfate[f]	1.15	0.30	1.87×10^{-29}	4.36×10^{-29}				
88	TG(24:1/22:6/22:6)[e]	1.03	1.67	3.63×10^{-10}	5.20×10^{-10}				

[a]VIP was obtained from OPLS-DA model with a threshold of 1.0. [b]FC was obtained by comparing those metabolites in patients with CKD with the healthy controls; FC with a value >1 indicated a relatively higher intensity presenting in patients with CKD, whereas a value <1 indicated a relatively lower intensity compared with the healthy controls. [c]*P* values from one-way ANOVA. [d]Value of FDR was obtained from the adjusted *P* value of FDR correction by Benjamini-Hochberg method. [e]Metabolites were predicted according to the MS and MS/MS using databases. [f]Metabolites validated with their analogue structure of authentic chemicals. [g]Metabolites validated with authentic chemicals.

mode, respectively. PCA score plots and the heatmap showed that 126 lipid species could separate patients with CKD from healthy controls (Figure S2). Having a $P < 0.05$ were 113 out of 126 lipid species based on one-way ANOVA and adjusted FDR. Subsequent analysis showed that 88 out of 113 lipid species had an AUC > 0.85 based on ROC analysis and 59, 19, and 10 lipids were identified by the MS and MS/MS using databases, analogue structure of authentic chemicals, and authentic chemicals, respectively (Table 2). PCA score plots and heatmap showed that 88 lipid species could separate patients with CKD from healthy controls (Figure 1). For the lipid species, 64 out of 113 have sensitivity and specificity equal to or greater than 85% (Table 2).

The potential relationships of the lipid species were analyzed using hierarchical clustering analyses. In accordance with their Pearson correlation coefficients, 64 lipid species and the closely associated lipids were clustered (Figure 2A). Three main lipid classes including glycerophospholipids (PC, PE, PG, LPC, and LPE), glycerolipids (MG, DG, and TG), and fatty acids were observed in four major clusters. Additionally, SAM was further used for lipid species selection.[24] SAM identified 54 altered lipid species (Figure 2B). To predict diagnostic performance for each sample, predicted class probabilities was performed on 71 lipid species (Figure 2C). All 120 serum samples from CKD were correctly grouped with 100% sensitivity. Data from all 80 control individuals were located in the control area with 100% specificity. Therefore, these lipid species were closely associated with abnormal lipid metabolism in patients with CKD. Significantly increased total fatty acids, glycerolipids, and glycerophospholipids were observed in patients with CKD compared to the healthy controls (Figure 3A). To further confirm the significant changes in serum profile with severity of CKD, we analyzed the relationships among total fatty acids, glycerolipids and glycerophospholipids, triglyceride (TG), and total cholesterol (TC) with eGFR in patients with CKD. The serum level of total fatty acids, glycerolipids, and glycerophospholipids directly correlated with serum TG and inversely correlated with the eGFR and TC (Figure 3, panels B to C). Figure 4 showed the intensities of 60 individual lipid species. Significant increases in 6 saturated fatty acids (SFA) and 14 glycerolipids as well as significant decreases in 7 polyunsaturated fatty-acids (PUFA) and 8 glycerolipids were observed in patients with CKD. Except for 1 PC and 1 LPC, 22 glycerophospholipids were significantly increased in patients with CKD.

3.3. BLR and ROC Curve Analysis

On the basis of the 64 differential lipid species, a logistic regression model was developed to assess the potential utility of significantly altered lipid species for the discrimination between patients with CKD and healthy controls. Through a forward stepwise analysis, methyl hexadecanoic acid, LPC(24:1), 3-oxo-octadecanoic acid, and PC(20:2/24:1) were identified as reliable lipid species in the regression model. Significantly increased methyl hexadecanoic acid, LPC(24:1), and 3-oxooctadecanoic acid and decreased PC(20:2/24:1) were observed in patients with CKD.

DOI: 10.1021/acs.jproteome.6b00956
J. Proteome Res. 2017, 16, 1566−1578

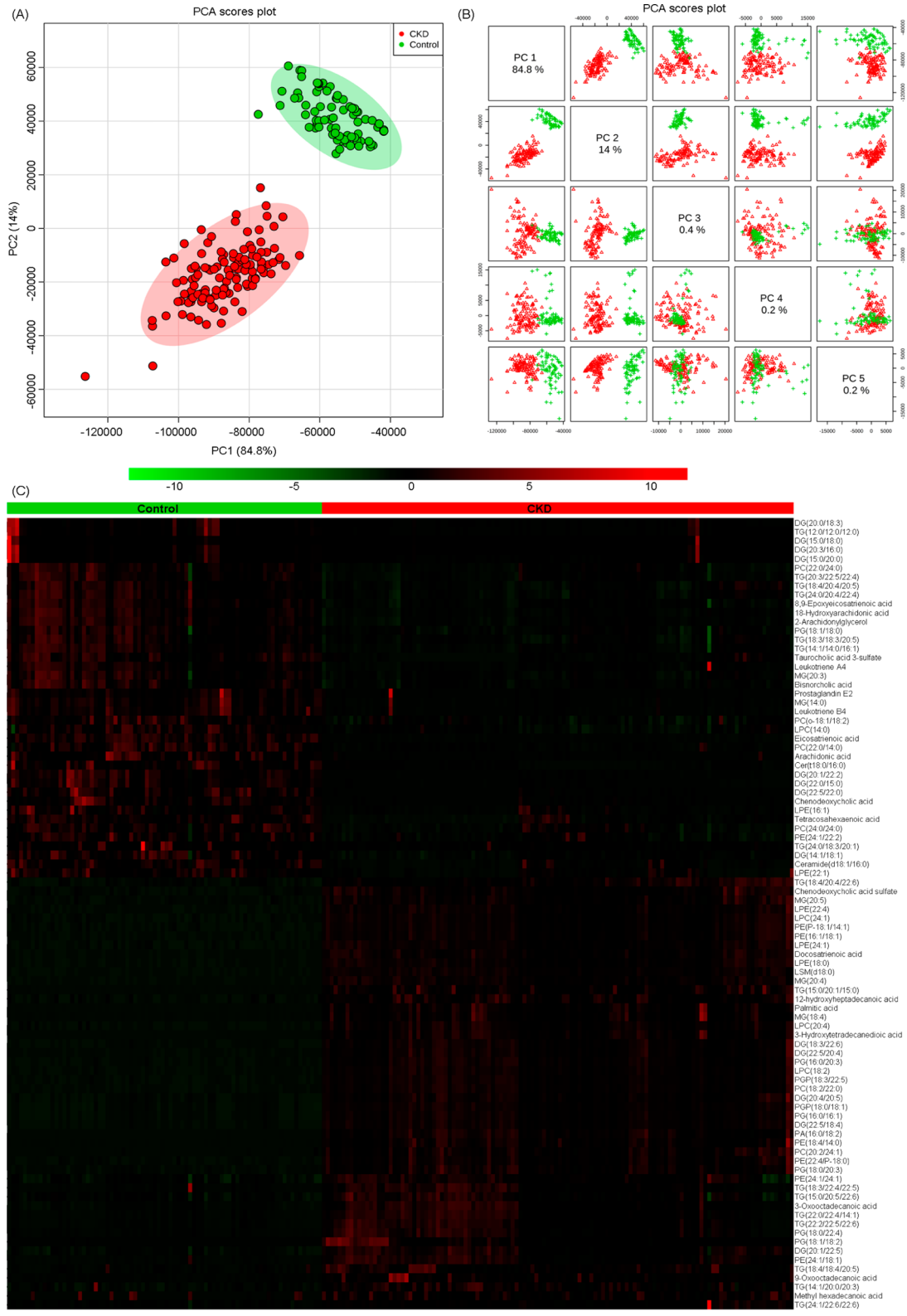

Figure 1. Lipidomic profiling of plasma samples from 88 lipid species from both positive ion mode and negative ion mode that distinguish patients with CKD from healthy controls. (A) PCA of two components of lipid species from 120 CKD samples and 80 control samples. (B) Different principal components have a different contribution to separating CKD from healthy controls in this study. Red triangles and green crosses represent patients with CKD and healthy controls, respectively. (C) Heatmap of altered lipid species between patients with CKD and healthy controls. Red and green indicate increased and decreased levels, respectively. Rows: lipid species; columns: plasma sample.

DOI: 10.1021/acs.jproteome.6b00956
J. Proteome Res. 2017, 16, 1566−1578

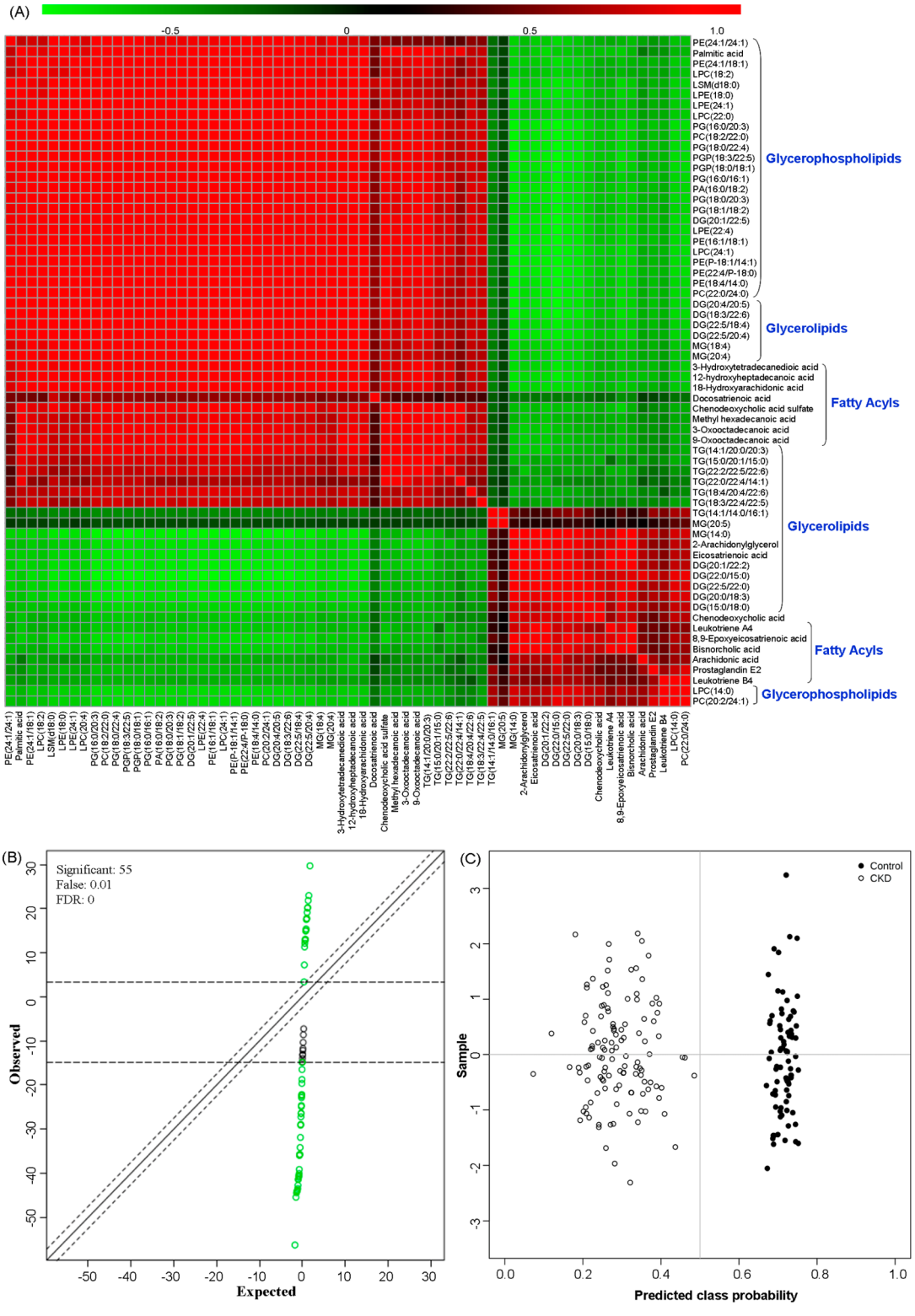

Figure 2. Analysis of Pearson correlation coefficients and diagnostic performances. (A) Hierarchical clustering analyses of the identified significant lipid species. Four clusters were identified, indicating the patients with CKD and healthy controls of lipid species. Pearson correlation coefficients of the seventy-one identified significant lipid species were shown on the plot. (B) The result of SAM scatter plot of observed scores plotted versus the expected scores with a delta value of 3.0. The diagonal solid line indicates where these two measures are the same, whereas the dotted lines indicate the significance threshold based on Delta = 3.0. The dotted lines are drawn at a distance of delta from the solid line. The significant lipid species are represented in green. The green open circles above and below the dotted lines correspond to the increased and decreased lipid intensities, respectively. (C) Diagnostic performances of the 71 differential lipid species based on the PLS-DA model.

DOI: 10.1021/acs.jproteome.6b00956
J. Proteome Res. 2017, 16, 1566−1578

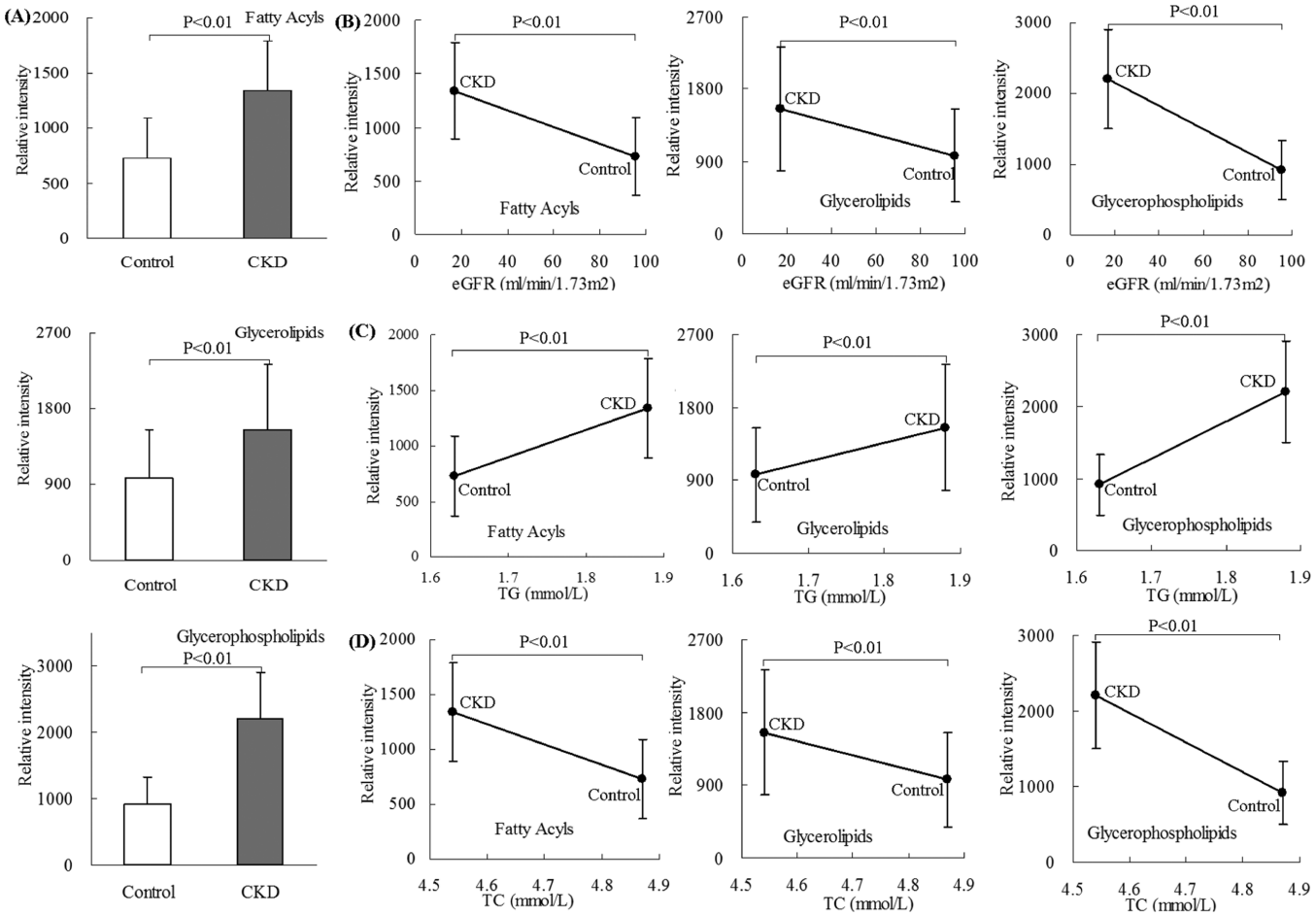

Figure 3. Intensity of total fatty acyls, glycerolipids, and glycerophospholipids were correlated with eGFR, TG, and TC. (A) Significantly increased total fatty acyls, glycerolipids, and glycerophospholipids. (B) Correlations between eGFR and the total fatty acyls, glycerolipids, and glycerophospholipids. (C) Correlations between triglyceride and the total fatty acyls, glycerolipids, and glycerophospholipids. (D) Correlations between total cholesterol and the total fatty acyls, glycerolipids, and glycerophospholipids.

3.4. Validation of Four Significantly Altered Lipid Species

For validation of four lipid species, these lipid species were measured in the serum of an independent cohort. The results confirmed that the four lipid species could separate patients with CKD from the healthy controls with high sensitivity, specificity, and diagnostic performances (Figure 5, panels A, B, and C). Diagnostic performances showed all 60 CKD samples were located in the CKD area (100% sensitivity) and 38 out of the 40 control samples were correctly grouped (95% specificity) (Figure 5D). Significantly increased methyl hexadecanoic acid, LPC(24:1) and 3-oxooctadecanoic acid and decreased PC(20:2/24:1) were observed in 60 patients with CKD compared to the 40 healthy controls (Figure 6A). To further validate candidates that might be useful in detecting CKD, we analyzed the relationship between each lipid species and eGFR and serum creatinine levels. The analysis showed that methyl hexadecanoic acid, LPC(24:1), and 3-oxooctadecanoic acid were inversely correlated while PC(20:2/24:1) were positively correlated with eGFR. Methyl hexadecanoic acid, LPC(24:1), and 3-oxooctadecanoic acid were positively correlated while PC(20:2/24:1) was inversely correlated with serum creatinine level. Figure 6 demonstrates the strong correlation between each lipid species and eGFR and serum creatinine ($R > 0.8758$).

4. DISCUSSION

In this study, we found significant increases in the serum levels of total fatty acids, glycerolipids, and glycerophospholipids in patients with CKD. The serum levels of total fatty acids, glycerolipids, and glycerophospholipids were positively correlated with the TG and inversely correlated with the eGFR and TC. In addition, we found significant increases in 7 fatty acids and 14 glycerolipids as well as significant decreases in 7 fatty acids and 8 glycerolipids in patients with CKD. Except for one PC and one LPC, twenty-two glycerophospholipids were significantly increased in patients with CKD. Increased methyl hexadecanoic acid, LPC(24:1), and 3-oxooctadecanoic acid levels as well as the decreased PC(20:2/24:1) level were chosen using BLR. These findings were confirmed using an independent cohort employed in the discovery phase.

Interestingly, our study showed that SFA levels were significantly increased while PUFA levels were significantly decreased in patients with CKD compared to the healthy controls. High levels of free fatty acids (FFA) and SFA are closely associated with a higher risk of cardiovascular disease in patients with CKD. Many studies have reported that the serum levels of FFA and SFA are significantly increased in patients with kidney disease. Increased serum FFA and SFA levels have

DOI: 10.1021/acs.jproteome.6b00956
J. Proteome Res. 2017, 16, 1566−1578

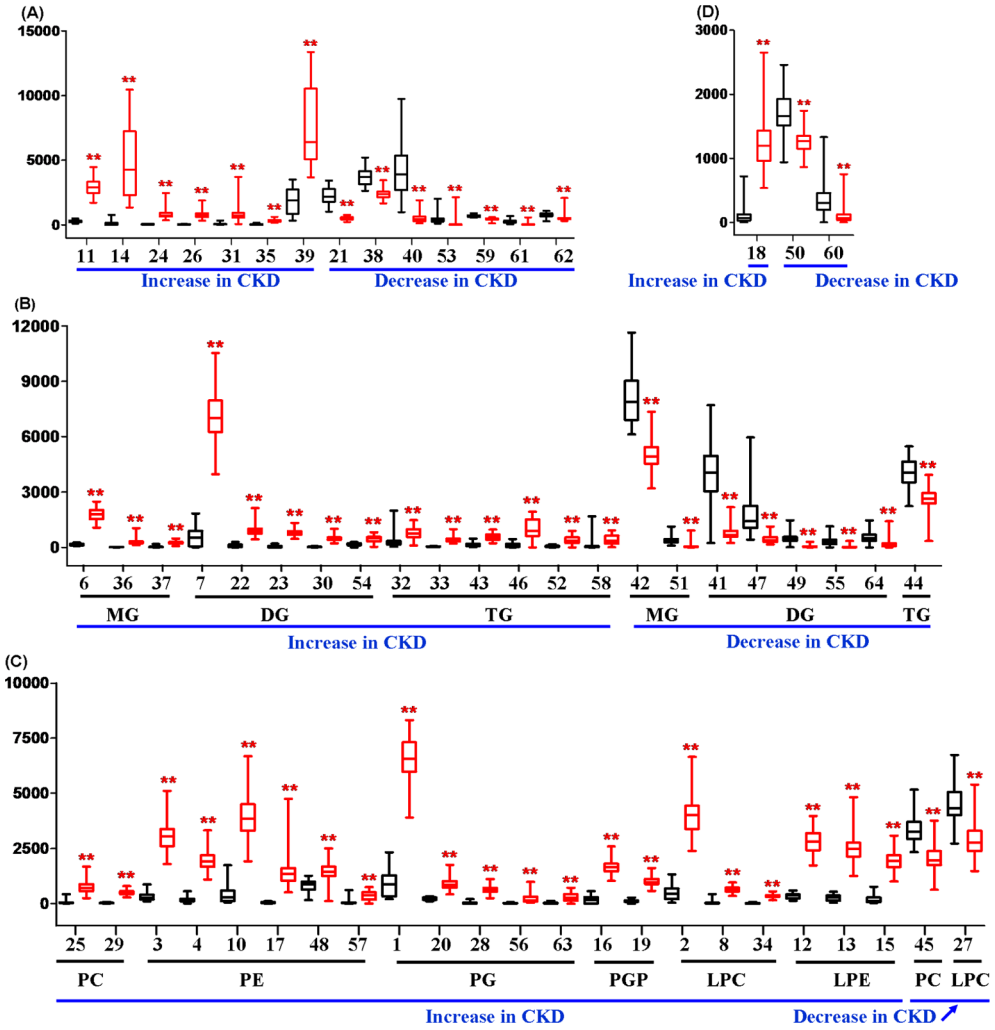

Figure 4. Box plots of major lipid species, including fatty acyls, glycerolipids, glycerophospholipids, and sterols in patients with CKD and healthy controls. Black and red boxes represent healthy controls and patients with CKD, respectively. The lines in the boxes represent the median intensity value for each lipid; the upper and lower boundaries of the box indicate the 75th and 25th percentiles, respectively; the upper and lower whiskers represent the maximum and minimum values. $^{**}P < 0.01$, compared with healthy controls.

been observed in the prehemodialysis patients compared to the healthy controls.[19] In fact, an increased serum SFA level has been shown to be associated with an increased risk of sudden cardiac death in hemodialysis patients.[25] Methyl hexadecanoic acid and 3-oxooctadecanoic acid are both SFA. Metabolomics study demonstrated that methyl hexadecanoic acid was identified from bronchoalveolar lavage fluid in preterm infants complicated by respiratory distress syndrome.[26] 3-Oxooctadecanoic acid was an intermediate product in fatty acid biosynthesis, and it was converted from malonic acid via the enzyme. In humans, fatty acids are mainly formed in the liver and adipose tissue and mammary glands. Recent metabolomics study showed that 3-oxohexadecanoic acid was an important metabolite in the saliva of the γ-irradiation-induced mice.[27] Our study showed that significant increased methyl hexadecanoic acid and 3-oxooctadecanoic acid levels were well-correlated with eGFR and serum creatinine in patients with CKD, which are consistent with the above-mentioned publications. Recently, Kang et al. demonstrated downregulation of key enzymes and regulators of fatty acid oxidation and increased intracellular lipid deposition in both humans and the mouse model with tubulointerstitial fibrosis.[6] Experiments using tubular epithelial cells indicated that inhibition of fatty acid oxidation causes ATP depletion, cell death, intracellular lipid deposition, and dedifferentiation to pro-fibrotic phenotype. In contrast, restoration of fatty acid metabolism by genetic or pharmacological manipulations protected mice from tubulointerstitial fibrosis.[6] Uptake of long-chain fatty acids is facilitated by the long-chain fatty acid transporter, CD36.[28] Metabolism of fatty acid requires their transport into the mitochondria by combining fatty acids to carnitine via carnitine palmitoyltransferase 1, which is the rate-limiting enzyme in fatty acid oxidation.[29] The β-oxidation of fatty acids takes place in the mitochondria, and reduced fatty acid oxidation results in mitochondrial dysfunction and oxidative phosphorylation defect.[6] Normally, fatty acid uptake, oxidation, and synthesis are tightly balanced to avoid intracellular lipid accumulation. Reduced thiobarbituric acid-reactive substance may limit oxidative stress by associating with the assembly of PUFA in membrane lipids and lipoproteins, making the double bonds less available for attack by free radicals; inhibiting the pro-oxidant enzyme, phospholipase A2; and by upregulating antioxidant enzymes.[30] Accumulated evidence indicated that fatty acid metabolism is disturbed in patients with CKD and contributes to the increased fatty acid peroxidation and development of oxidative stress.

DOI: 10.1021/acs.jproteome.6b00956
J. Proteome Res. 2017, 16, 1566−1578

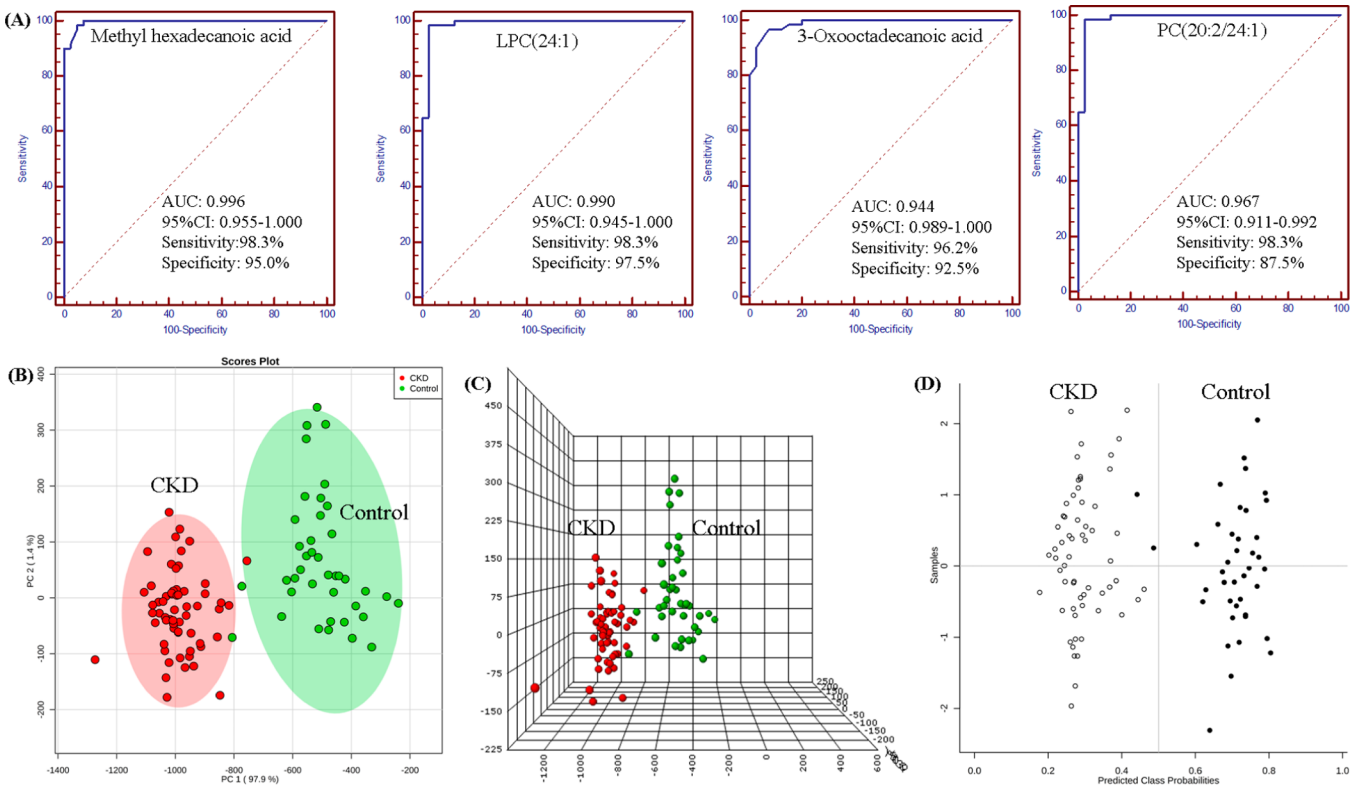

Figure 5. Validations of biomarker from multivariate statistical analyses. (A) PLS-DA-based ROC curves for the diagnosis power of four plasma individual lipids for distinguishing CKD from healthy controls. The four lipids have an AUC value of more than 0.85 and high sensitivity and specificity. They could potentially be considered as predictive lipids for CKD. The (B) 2D PCA and (C) 3D PCA score scatter plot using four lipids from 60 patients with CKD and 40 healthy controls. The unsupervised PCA score plots showed that four lipids could separate patients with CKD from the healthy controls. (D) Diagnostic performances of the four lipids in plasma based on the PLS-DA model from 60 patients with CKD and 40 healthy controls. All 60 CKD samples were located in the CKD area (100% sensitivity). Out of the 40 control samples, 38 were correctly grouped (95% specificity).

Elevated triglyceride level is associated with cardiovascular and all-cause mortality. The metabolism of glycerolipids including MG, DG, and TG are disturbed in patients with CKD. Previous studies have found significant alterations in glycerolipids synthesis and catabolism in patients with renal cell carcinoma and CKD.[18,31] Most of the previous studies have mainly measured total TG level in patients with CKD. In the present study, we found elevated levels of 6 TG and decreased level of one TG in patients with CKD. Reis et al. found that although total LDL was unaltered, triglyceride level of LDL was significantly increased in patients with CKD.[20] Elevation of TG is commonly accompanied by significant reduction of high-density lipoprotein cholesterols in patients with CKD.[32] Serum triglycerides are significantly increased in patients and animals with CKD. Hypertriglyceridemia in CKD is primarily due to impaired TG clearance occasioned by down-regulations of lipoprotein lipase and VLDL receptor in adipose tissues and skeletal muscles and hepatic lipase and LDL receptor related protein in the liver.[33,34] Five DG were increased and five DG were decreased in patients with CKD in our study. Teramoto et al. reported that 3-month ingestion of exogenous DG reduced the level of abdominal fat and improved serum lipid profile in free-living hemodialysis patients. Ingestion of DAG significantly decreased serum VLDL, altered serum MG, and increased high-density lipoprotein (HDL) levels at three months.[35]

Glycerophospholipids are the main components of the cell membranes and play a major role in cell signaling, membrane anchoring, and substrate transport. Serum levels of 22 glycerophospholipids including PC, PE, LPC, LPE, and PGP were significantly altered in our patients with CKD. Previous studies have demonstrated abnormal glycerophospholipids in patients and animals with CKD.[18,36−39] For example, abnormal PC metabolism was observed in patients with mild to advanced CKD.[40] In addition, Rhee et al. have reported decreased LPC including LPC(18:1) and LPC(18:2) in advanced patients with CKD and decreased LPC(14:0), PC(34:4), PC(32:2), and PC(38:3) in patients with ESRD.[41,42] Phospholipases can catalyze the decomposition of phospholipids to release FFA. Therefore, activation of phospholipase A2 can lead to the release of FFA, reduction of PC, and elevation of the LPC levels. These are consistent with the results of the present study which revealed significant decrease in PC(20:2/24:1) coupled with significant increases in LPC(24:1) and FFA levels in our patients with CKD. In addition, LPC is produced from PC by lecithin cholesterol acyltransferase.[43] Lee et al. demonstrated that hemodialysis patients with low LPC level have a higher risk of cardiovascular disease than those with higher LPC level.[44] Decrease in PC(20:2/24:1) and increase in LPC(24:1) are consistent with previously demonstrated deficiency of lecithin cholesterol acyltransferase and activation of phospholipase A2 in patients with CKD.[45]

The main limitations of the present study are limited number of patients which precluded the ability to explore the impact of gender, age, nutritional status, systemic inflammation, and use of various drugs on the observed abnormalities of lipid metabolites in our patients with CKD.

DOI: 10.1021/acs.jproteome.6b00956
J. Proteome Res. 2017, 16, 1566−1578

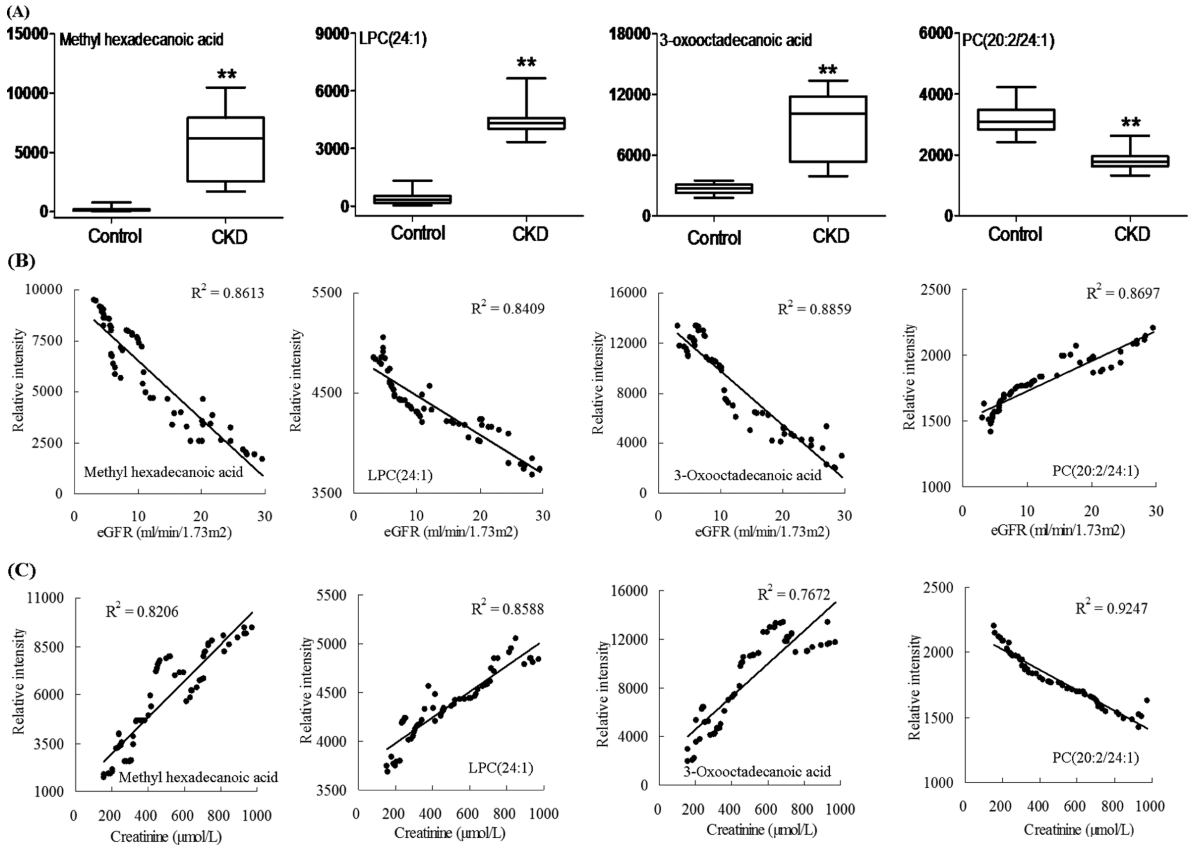

Figure 6. Validations of biomarker by using correlation between plasma four lipid levels and eGFR and creatinine. (A) Box and whisker plots indicating the levels of methyl hexadecanoic acid, LPC(24:1), 3-oxooctadecanoic acid, and PC(20:2/24:1) in CKD versus healthy controls. The lines in the boxes represent the median intensity value for each lipid; the upper and lower boundaries of the box indicate the 75th and 25th percentiles, respectively; the upper and lower whiskers represent the maximum and minimum values. $^{**}P < 0.01$, compared with healthy controls. (B) Correlation between methyl hexadecanoic acid, LPC(24:1), 3-oxooctadecanoic acid, and PC(20:2/24:1) levels (peak intensity) measured by the UPLC-MS and eGFR by calculated formula. (C) Correlation between methyl hexadecanoic acid, LPC(24:1), 3-oxooctadecanoic acid, and PC(20:2/24:1) levels (peak intensity) measured by the UPLC-MS and creatinine (μmol/L) measured by the clinical laboratory. The horizontal axes show the eGFR value or creatinine level. The vertical axis shows the peak intensity of each plasma sample. The correlation coefficient is shown in each graph.

5. CONCLUSIONS

A UPLC-HDMS-based lipidomic approach was used to analyze serum lipids in advanced patients with CKD. Significantly increased methyl hexadecanoic acid, LPC(24:1), and 3-oxo-octadecanoic acid and significantly decreased PC(20:2/24:1) strongly correlated with eGFR and the creatinine level. These lipid metabolites were significantly altered in serum samples of patients with advanced CKD of different etiology. Application of UPLC-HDMS-based lipidomic technique revealed profound changes in lipid metabolites in patients with advanced CKD.

■ ASSOCIATED CONTENT

Supporting Information

The Supporting Information is available free of charge on the ACS Publications website at DOI: 10.1021/acs.jproteome.6b00956.

Figure S1: multivariate analysis of OPLS-DA. Scores scatter plot for OPLS-DA showed that patients with CKD could be separated from healthy controls in (A) positive ion mode and (B) negative ion mode indicating that serum lipid metabolic patterns were significantly altered in patients with CKD. Blue and green dots represent patients with CKD and healthy controls, respectively. From S-plots, 287 and 196 variables were selected according to the VIP values from S-plots in (C) positive ion mode and (D) negative ion mode, respectively. Figure S2: lipidomic profiling from 126 lipid metabolites can distinguish patients with CKD from healthy controls. (A) PCA score plots showed that 126 lipid species could separate patients with CKD from healthy controls. (B) Patients with CKD could be separated from healthy controls in different principal components. Red triangles and green crosses represent patients with CKD and healthy controls, respectively. (C) Heatmap of differential lipid metabolites between patients with CKD and healthy controls. Lipid dysregulation was observed in patients with CKD compared to the healthy controls. Red and green indicate increased and decreased levels, respectively (PDF)

■ AUTHOR INFORMATION

Corresponding Author

*E-mail: zyy@nwu.edu.cn and zhaoyybr@163.com. Tel.: +86 29 88305273. Fax: +86 29 88303572.

ORCID

Ying-Yong Zhao: 0000-0002-0239-7342

Notes

The authors declare no competing financial interest.

[@]H.C. and L.C. are cofirst authors.

DOI: 10.1021/acs.jproteome.6b00956
J. Proteome Res. 2017, 16, 1566−1578

■ ACKNOWLEDGMENTS

This study was supported by the National Natural Science Foundation of China (Grants 81673578 and 81603271), the Program for the New Century Excellent Talents in University from Ministry of Education of China (Grant NCET-13-0954), and the project As a Major New Drug to Create a Major National Science and Technology Special (Grant 2014ZX09304307-002).

■ REFERENCES

(1) Chawla, L. S.; Eggers, P. W.; Star, R. A.; Kimmel, P. L. Acute kidney injury and chronic kidney disease as interconnected syndromes. *N. Engl. J. Med.* **2014**, *371*, 58−66.

(2) Chen, H.; Cao, G.; Chen, D. Q.; Wang, M.; Vaziri, N. D.; Zhang, Z. H.; Mao, J. R.; Bai, X.; Zhao, Y. Y. Metabolomics insights into activated redox signaling and lipid metabolism dysfunction in chronic kidney disease progression. *Redox Biol.* **2016**, *10*, 168−178.

(3) Vaziri, N. D. Lipotoxicity and impaired high density lipoprotein-mediated reverse cholesterol transport in chronic kidney disease. *J. Renal Nutr.* **2010**, *20*, S35−43.

(4) Zhao, Y. Y.; Cheng, X. L.; Vaziri, N. D.; Liu, S.; Lin, R. C. UPLC-based metabonomic applications for discovering biomarkers of diseases in clinical chemistry. *Clin. Biochem.* **2014**, *47*, 16−26.

(5) Chen, D. Q.; Chen, H.; Chen, L.; Vaziri, N. D.; Wang, M.; Li, X. R.; Zhao, Y. Y. The link between phenotype and fatty acid metabolism in advanced chronic kidney disease. *Nephrol., Dial., Transplant.* **2017**, DOI: 10.1093/ndt/gfw415.

(6) Kang, H. M.; Ahn, S. H.; Choi, P.; Ko, Y. A.; Han, S. H.; Chinga, F.; Park, A. S.; Tao, J.; Sharma, K.; Pullman, J.; Bottinger, E. P.; Goldberg, I. J.; Susztak, K. Defective fatty acid oxidation in renal tubular epithelial cells has a key role in kidney fibrosis development. *Nat. Med.* **2014**, *21*, 37−46.

(7) Zhang, Z. H.; Chen, H.; Vaziri, N. D.; Mao, J. R.; Zhang, L.; Bai, X.; Zhao, Y. Y. Metabolomic signatures of chronic kidney disease of diverse etiologies in the rats and humans. *J. Proteome Res.* **2016**, *15*, 3802−3812.

(8) Vaziri, N. D. Dyslipidemia of chronic renal failure: The nature, mechanisms and potential consequences. *Am. J. Physiol.: Renal, Fluid Electrolyte Physiol.* **2006**, *290*, F262−F272.

(9) Vaziri, N. D. Molecular mechanisms of lipid dysregulation in nephrotic syndrome. *Kidney Int.* **2003**, *63*, 1964−76.

(10) Vaziri, N. D. Disorders of lipid metabolism in nephrotic syndrome: mechanisms and consequences. *Kidney Int.* **2016**, *90*, 41−52.

(11) Zhao, Y. Y.; Cheng, X. L.; Lin, R. C. Lipidomics applications for discovering biomarkers of diseases in clinical chemistry. *Int. Rev. Cell Mol. Biol.* **2014**, *313*, 1−26.

(12) Spickett, C. M.; Pitt, A. R. Oxidative lipidomics coming of age: advances in analysis of oxidized phospholipids in physiology and pathology. *Antioxid. Redox Signaling* **2015**, *22*, 1646−66.

(13) Zhao, Y. Y.; Wu, S. P.; Liu, S.; Zhang, Y.; Lin, R. C. Ultra-performance liquid chromatography-mass spectrometry as a sensitive and powerful technology in lipidomic applications. *Chem.-Biol. Interact.* **2014**, *220*, 181−92.

(14) Castro-Perez, J. M.; Kamphorst, J.; DeGroot, J.; Lafeber, F.; Goshawk, J.; Yu, K.; Shockcor, J. P.; Vreeken, R. J.; Hankemeier, T. Comprehensive LC-MS^E lipidomic analysis using a shotgun approach and its application to biomarker detection and identification in osteoarthritis patients. *J. Proteome Res.* **2010**, *9*, 2377−89.

(15) Rainville, P. D.; Stumpf, C. L.; Shockcor, J. P.; Plumb, R. S.; Nicholson, J. K. Novel application of reversed-phase UPLC-oaTOF-MS for lipid analysis in complex biological mixtures: A new tool for lipidomics. *J. Proteome Res.* **2007**, *6*, 552−8.

(16) Zhang, Z. H.; Vaziri, N. D.; Wei, F.; Cheng, X. L.; Bai, X.; Zhao, Y. Y. An integrated lipidomics and metabolomics reveal nephroprotective effect and biochemical mechanism of *Rheum officinale* in chronic renal failure. *Sci. Rep.* **2016**, *6*, 22151.

(17) Zhao, Y. Y.; Wang, H. L.; Cheng, X. L.; Wei, F.; Bai, X.; Lin, R. C.; Vaziri, N. D. Metabolomics analysis reveals the association between lipid abnormalities and oxidative stress, inflammation, fibrosis, and Nrf2 dysfunction in aristolochic acid-induced nephropathy. *Sci. Rep.* **2015**, *5*, 12936.

(18) Zhao, Y. Y.; Vaziri, N. D.; Lin, R. C. Lipidomics: new insight into kidney disease. *Adv. Clin. Chem.* **2015**, *68*, 153−75.

(19) Wang, L.; Hu, C.; Liu, S.; Chang, M.; Gao, P.; Wang, L.; Pan, Z.; Xu, G. Plasma lipidomics investigation of hemodialysis effects by using liquid chromatography-mass spectrometry. *J. Proteome Res.* **2016**, *15*, 1986−94.

(20) Reis, A.; Rudnitskaya, A.; Chariyavilaskul, P.; Dhaun, N.; Melville, V.; Goddard, J.; Webb, D. J.; Pitt, A. R.; Spickett, C. M. Top-down lipidomics of low density lipoprotein reveal altered lipid profiles in advanced chronic kidney disease. *J. Lipid Res.* **2015**, *56*, 413−22.

(21) Miao, H.; Zhao, Y. H.; Vaziri, N. D.; Tang, D. D.; Chen, H.; Chen, H.; Khazaeli, M.; Tarbiat-Boldaji, M.; Hatami, L.; Zhao, Y. Y. Lipidomics biomarkers of diet-induced hyperlipidemia and its treatment with *Poria cocos*. *J. Agric. Food Chem.* **2016**, *64*, 969−79.

(22) Zhao, Y. Y.; Cheng, X. L.; Wei, F.; Bai, X.; Tan, X. J.; Lin, R. C.; Mei, Q. Intrarenal metabolomic investigation of chronic kidney disease and its TGF-β1 mechanism in induced-adenine rats using UPLC Q-TOF/HSMS/MS^E. *J. Proteome Res.* **2013**, *12*, 692−703.

(23) Zhao, Y. Y.; Liu, J.; Cheng, X. L.; Bai, X.; Lin, R. C. Urinary metabonomics study on biochemical changes in an experimental model of chronic renal failure by adenine based on UPLC Q-TOF/MS. *Clin. Chim. Acta* **2012**, *413*, 642−49.

(24) Larsson, O.; Wahlestedt, C.; Timmons, J. A. Considerations when using the significance analysis of microarrays (SAM) algorithm. *BMC Bioinf.* **2005**, *6*, 129.

(25) Friedman, A. N.; Yu, Z.; Denski, C.; Tamez, H.; Wenger, J.; Thadhani, R.; Li, Y.; Watkins, B. Fatty acids and other risk factors for sudden cardiac death in patients starting hemodialysis. *Am. J. Nephrol.* **2013**, *38*, 12−8.

(26) Fabiano, A.; Gazzolo, D.; Zimmermann, L. J.; Gavilanes, A. W.; Paolillo, P.; Fanos, V.; Caboni, P.; Barberini, L.; Noto, A.; Atzori, L. Metabolomic analysis of bronchoalveolar lavage fluid in preterm infants complicated by respiratory distress syndrome: preliminary results. *J. Matern.-Fetal Neonat. Med.* **2011**, *24*, 55−58.

(27) Laiakis, E. C.; Strawn, S. J.; Brenner, D. J.; Fornace, A. J., Jr. Assessment of saliva as a potential biofluid for biodosimetry: A pilot metabolomics study in mice. *Radiat. Res.* **2016**, *186*, 92−97.

(28) Susztak, K.; Ciccone, E.; McCue, P.; Sharma, K.; Böttinger, E. P. Multiple metabolic hits converge on CD36 as novel mediator of tubular epithelial apoptosis in diabetic nephropathy. *PLoS Med.* **2005**, *2*, e45.

(29) Schug, T. T.; Li, X. Sirtuin 1 in lipid metabolism and obesity. *Ann. Med.* **2011**, *43*, 198−211.

(30) Suresh, D. R.; Delphine, S.; Agarwal, R. Biochemical markers of oxidative stress in predialytic chronic renal failure patients. *Hong Kong J. Nephrol.* **2008**, *10*, 69−73.

(31) Cheng, Y.; Hong, M.; Cheng, B. Identified differently expressed genes in renal cell carcinoma by using multiple microarray datasets running head: differently expressed genes in renal cell carcinoma. *Eur. Rev. Med. Pharmacol. Sci.* **2014**, *18*, 1033−1040.

(32) Piperi, C.; Kalofoutis, C.; Tzivras, M.; Troupis, T.; Skenderis, A.; Kalofoutis, A. Effects of hemodialysis on serum lipids and phospholipids of end-stage renal failure patients. *Mol. Cell. Biochem.* **2004**, *265*, 57−61.

(33) Vaziri, N. D.; Yuan, J.; Ni, Z.; Nicholas, S. B.; Norris, K. C. Lipoprotein lipase deficiency in chronic kidney disease is compounded by downregulation of endothelial GPIHBP1 expression. *Clin. Exp. Nephrol.* **2012**, *16*, 238−43.

(34) Kim, C.; Vaziri, N. D. Downregulation of hepatic LDL receptor-related protein (LRP) in chronic renal failure. *Kidney Int.* **2005**, *67*, 1028−32.

(35) Teramoto, T.; Watanabe, H.; Ito, K.; Omata, Y.; Furukawa, T.; Shimoda, K.; Hoshino, M.; Nagao, T.; Naito, S. Significant effects of

DOI: 10.1021/acs.jproteome.6b00956
J. Proteome Res. 2017, 16, 1566−1578

diacylglycerol on body fat and lipid metabolism in patients on hemodialysis. *Clin. Nutr.* **2004**, *23*, 1122−1126.
(36) Zhao, Y. Y. Metabolomics in chronic kidney disease. *Clin. Chim. Acta* **2013**, *422*, 59−69.
(37) Rhee, E. P. Metabolomics and renal disease. *Curr. Opin. Nephrol. Hypertens.* **2017**, *24*, 371−379.
(38) Ye, L.; Mao, W. Metabonomic biomarkers for risk factors of chronic kidney disease. *Int. Urol. Nephrol.* **2016**, *48*, 547−52.
(39) Barrios, C.; Spector, T. D.; Menni, C. Blood, urine and faecal metabolite profiles in the study of adult renal disease. *Arch. Biochem. Biophys.* **2016**, *589*, 81−92.
(40) Nkuipou-Kenfack, E.; Duranton, F.; Gayrard, N.; Argilés, À.; Lundin, U.; Weinberger, K. M.; Dakna, M.; Delles, C.; Mullen, W.; Husi, H.; Klein, J.; Koeck, T.; Zürbig, P.; Mischak, H. Assessment of metabolomic and proteomic biomarkers in detection and prognosis of progression of renal function in chronic kidney disease. *PLoS One* **2014**, *9*, e96955.
(41) Rhee, E. P.; Clish, C. B.; Ghorbani, A.; Larson, M. G.; Elmariah, S.; McCabe, E.; Yang, Q.; Cheng, S.; Pierce, K.; Deik, A.; Souza, A. L.; Farrell, L.; Domos, C.; Yeh, R. W.; Palacios, I.; Rosenfield, K.; Vasan, R. S.; Florez, J. C.; Wang, T. J.; Fox, C. S.; Gerszten, R. E. A combined epidemiologic and metabolomic approach improves CKD prediction. *J. Am. Soc. Nephrol.* **2013**, *24*, 1330−8.
(42) Rhee, E. P.; Souza, A.; Farrell, L.; Pollak, M. R.; Lewis, G. D.; Steele, D. J.; Thadhani, R.; Clish, C. B.; Greka, A.; Gerszten, R. E. Metabolite profiling identifies markers of uremia. *J. Am. Soc. Nephrol.* **2010**, *21*, 1041−51.
(43) Rye, K. A.; Barter, P. J. Regulation of high-density lipoprotein metabolism. *Circ. Res.* **2014**, *114*, 143−56.
(44) Lee, Y. K.; Lee, D. H.; Kim, J. K.; Park, M. J.; Yan, J. J.; Song, D. K.; Vaziri, N. D.; Noh, J. W. Lysophosphatidylcholine, oxidized low-density lipoprotein and cardiovascular disease in Korean hemodialysis patients: analysis at 5 years of follow-up. *J. Korean Med. Sci.* **2013**, *28*, 268−73.
(45) Calabresi, L.; Simonelli, S.; Conca, P.; Busnach, G.; Cabibbe, M.; Gesualdo, L.; Gigante, M.; Penco, S.; Veglia, F.; Franceschini, G. Acquired lecithin: cholesterol acyltransferase deficiency as a major factor in lowering plasma HDL levels in chronic kidney disease. *J. Intern. Med.* **2015**, *277*, 552−61.

DOI: 10.1021/acs.jproteome.6b00956
J. Proteome Res. 2017, 16, 1566−1578